

MODELING CELL MOVEMENT IN ANISOTROPIC AND HETEROGENEOUS NETWORK TISSUES

A. CHAUVIERE[†], T. HILLEN[‡] AND L. PREZIOSI[†]

[†]Politecnico di Torino
Corso Duca degli Abruzzi, 24
Torino 10129, Italy

[‡]University of Alberta
Edmonton, Canada T6G 2G1

(Communicated by Roberto Natalini)

ABSTRACT. Cell motion and interaction with the extracellular matrix is studied deriving a kinetic model and considering its diffusive limit. The model takes into account the chemotactic and haptotactic effects, and obtains friction as a result of the interactions between cells and between cells and the fibrous environment. The evolution depends on the fibre distribution, as cells preferentially move along the fibre direction and tend to cleave and remodel the extracellular matrix when their direction of motion is not aligned with the fibre direction. Simulations are performed to describe the behavior of an ensemble of cells under the action of a chemotactic field and in the presence of heterogeneous and anisotropic fibre networks.

Introduction. From recent experimental studies, much has been learned about cell movement in tissues (see, e.g., the work by Friedl and coworkers [16, 17, 18, 29]). Cells that move through tissues (like cancer metastases, or fibroblasts) interact with the tissue matrix as well as with other cells. Many different biological and physical processes intervene in a complicated way and a crucial role is played by the interactions between cells and Extra Cellular Matrix (ECM) [2, 9, 10, 11, 12].

In this paper we use a kinetic approach to derive continuum models for mass, momentum and energy. The model takes into account the phenomena like chemotaxis and haptotaxis, while it obtains friction stemming out naturally in the momentum equation from the interaction between cells and between them and the extracellular matrix. A continuum model describing the balance of mass, momentum and energy is obtained by writing the conservation equations related to the kinetic model and a diffusion limit is performed to obtain the final anisotropic advection-diffusion model. Cell-extracellular matrix interactions depend on the amount of extracellular matrix and on the fibre distribution, so that cells preferentially move along the fibre direction. The model also includes ECM cleavage by the cells, which particularly occurs when cell motion and fibre direction are not aligned.

2000 *Mathematics Subject Classification.* 92C17.

Key words and phrases. Mathematical model, Cell motion, Fiber network.

[†] The work has been partially funded by the MC-RTN Project MRTN-CT-2004-503661 “Modelling, mathematical methods and computer simulation for tumour growth and therapy”.

[‡] This work was supported by the Natural Science and Engineering Research Council of Canada.

This work generalizes an earlier model by Hillen [21] where a transport equation for moving cells was derived which includes cell-ECM interactions but does not include external actions and cell-cell interactions. Different transport models dealing with cell orientation are given in [10, 12, 13, 14].

The conservation equations derived here closely resemble those present in the models proposed in Gamba et al. [19] and Serini et al. [26], reviewed in Ambrosi et al. [3], to describe network formation by the motion of endothelial cells. In [23] this model was generalized to include an exogenous chemoattractant and chemorepellent to control the formation of vascular networks, while Tosin et al. [27] included the mechanical interaction with the homogeneous substratum using a continuum mechanics approach.

The paper is organized as follows: In the next section we describe our most general transport model for cell movement in tissues, including chemotaxis, cell-ECM interactions, contact guidance from network fibres and cell-cell interactions. The macroscopic quantities able to model the cell population and the fibrous medium are also introduced according to the statistical representation at the mesoscopic scale for these two populations.

In Section 2 we derive the system of moment equations for mass, momentum and energy. While mass is preserved, the momentum and energy equations present dissipation terms due to the interactions between the two populations modeled at the microscopic level.

In Section 3 we develop a specific example of cell movement in network tissue, modeling the interactions used in the transport equations. These interactions are introduced in the general case and then particularized: after having interacted among them, cells are assumed to choose a new velocity at random, while we assume that cells tend to align with the direction of the fibres they encounter. Drag forces and energy dissipation appearing in the moment equations are explicitly obtained.

As a way to close the system, we propose the diffusion limit of the transport equation in Section 4, and obtain a single advection-diffusion equation over the cell density.

We show in Section 5 how both approaches may be closed by the knowledge of the distribution function at the equilibrium, to derive finally the continuum model for mesenchymal motion in Section 6, including fibre network remodeling.

Numerical simulations are presented in the last section to emphasize the influence of the inhomogeneities and the anisotropy of the ECM on the cell motion. After checking that the cell distribution tends to the stationary analytical one for large time, in particular it is shown how cells peek near regions with denser ECM and tend to circumvent these regions. In the anisotropic case it is shown how cells move preferentially along the fibres, and how they prefer to choose the path with fibres that are along the direction they want to go in because of chemotaxis.

1. The cell movement model. We derive a general model for cells moving in a fibrous tissue that includes cell-fibre interactions, cell-cell interactions, chemotaxis and also the dynamics of the fibre network due to fibre degradation. The model is an extension of Hillen's M^5 -model [21], where only cell-fibre and fibre-cell interactions were included. In this paper we will explicitly refer to the three-dimensional case with the aim to describe the motion in an *in vivo* ECM. However, the two-dimensional case corresponding to the *in vitro* motion over a substratum can be worked out in a similar fashion.

The major players of the model are the cell population, the ECM fibre network and the chemotactic signal concentration. The statistical description of the cells is given by the distribution density function $p = p(t, \mathbf{x}, \mathbf{v})$, at time $t > 0$, location $\mathbf{x} \in \mathcal{D} \subseteq \mathbb{R}^3$ and velocity $\mathbf{v} \in V \subseteq \mathbb{R}^3$. In particular, p is normalized with respect to the total number of cells, so that $\int_{\mathcal{D}} \int_V p(t = 0, \mathbf{x}, \mathbf{v}) d\mathbf{x} d\mathbf{v} = 1$. Actually, since our model preserves mass, then $\int_{\mathcal{D}} \int_V p(t, \mathbf{x}, \mathbf{v}) d\mathbf{x} d\mathbf{v} = 1$ for all t . Often we will write the velocity vector as $\mathbf{v} = v\hat{\mathbf{v}}$ where $\hat{\mathbf{v}}$ defines the velocity direction and $v = |\mathbf{v}|$ the speed.

As far as the evolution of the extracellular matrix is concerned, we assume the collagen fibres to be rigid and degradable by the proteolytic activity of the cells to open their way through the extracellular matrix. The density and orientation of the fibrous ECM is given by the distribution density function $m = m(t, \mathbf{x}, \mathbf{n})$ where $\mathbf{n} \in S_+^2$ is a unit vector representing the angle defined over a half sphere, e.g., $z \geq 0$. The definition of m over the half sphere corresponds to the observation that fibres are not directional. Therefore, giving the distribution of fibres over half of the sphere completely characterizes how the fibres are placed. In the following, however, it will be useful to extend m over the entire unit sphere as an even function of \mathbf{n} by introducing the function

$$m^e(t, \mathbf{x}, \mathbf{n}) = \begin{cases} m(t, \mathbf{x}, \mathbf{n}) & \text{for } \mathbf{n} \in S_+^2, \\ m(t, \mathbf{x}, -\mathbf{n}) & \text{for } \mathbf{n} \in S_-^2. \end{cases} \tag{1}$$

The function m is also normalized, with respect to the total number of fibres at time $t = 0$ so that $\int_{\mathcal{D}} \int_{S_+^2} m(t = 0, \mathbf{x}, \mathbf{n}) d\mathbf{x} d\mathbf{n} = 1$. At a point $\mathbf{x} \in \mathcal{D}$ the total fibre density is denoted by

$$M(t, \mathbf{x}) = \int_{S_+^2} m(t, \mathbf{x}, \mathbf{n}) d\mathbf{n} = \frac{1}{2} \int_{S^2} m^e(t, \mathbf{x}, \mathbf{n}) d\mathbf{n}. \tag{2}$$

The orientation of the network can be described by its variance-covariance matrix. In fact, due to symmetry we find for the mean value

$$\int_{S^2} m^e(t, \mathbf{x}, \mathbf{n}) \mathbf{n} d\mathbf{n} = \mathbf{0}, \tag{3}$$

and the variance is given by the symmetric and positive definite tensor

$$\mathbb{D}(t, \mathbf{x}) = \frac{3}{M(t, \mathbf{x})} \int_{S_+^2} m(t, \mathbf{x}, \mathbf{n}) \mathbf{n} \otimes \mathbf{n} d\mathbf{n}, \tag{4}$$

also called orientation tensor, e.g. Tranquillo and Barocas [28]. In order to visualize it, it is useful to refer to the ellipsoid $\mathbf{x} \cdot \mathbb{D}\mathbf{x} = 1$ which has the axes identified by the eigenvectors of the tensor \mathbb{D} and gives the principal directions of the orientation of the network. In particular, in the isotropic case the tensor is diagonal and all eigenvalues are equal to 1. On the contrary, in the anisotropic case, the direction of the eigenvector corresponding to the maximum eigenvalue (e.g. the smallest axis of the ellipsoid) gives the main fibre direction. In the limit case in which the fibres are all aligned along the orientation \mathbf{N} , then $\mathbb{D} = 3\mathbf{N} \otimes \mathbf{N}$, the eigenvalues are 3 and 0 corresponding, respectively, to the eigenvector \mathbf{N} and to any orthogonal eigendirection. The ellipsoid is given by $(\mathbf{x} \cdot \mathbf{N})^2 = 1/3$, e.g., if $\mathbf{N} = \mathbf{e}_x$, it becomes simply $x = \pm 1/\sqrt{3}$. It is also useful to observe that $\text{tr}(\mathbb{D}) = 3$ in any case.

In this paper, we will deal with the evolution equation for m in Section 6. On the contrary, the chemotactic signal whose concentration is denoted by $\mathcal{C}(t, \mathbf{x})$, is assumed to be a given function of space and time. Adding another equation to describe the dynamics of the chemical is a technical extension.

To derive a transport model for cell movement we make the following assumptions:

- A1:** The net effect of chemotaxis is modeled as a force $\mathbf{f}(\mathcal{C}) \in \mathbb{R}^3$ depending on the given chemical profile $\mathcal{C}(t, \mathbf{x})$ and on its gradient. As an example we consider $\mathbf{f}(\mathcal{C}) = \lambda \nabla_{\mathbf{x}} \mathcal{C}$ where λ could also depend on \mathcal{C} .
- A2:** Cells can interact with the ECM both mechanically and chemically. The cells use fibres for contact guidance and also modify the network through degradation of collagen fibres by proteases. For the general theory the linear interaction operator of cells and ECM is denoted by J_m . We always assume cell mass conservation so that $\int_V J_m d\mathbf{v} = 0$.
- A3:** Cells interact with cells in a way where only mass is conserved during collisions. The quadratic cell-cell interaction operator is denoted by J_c which verifies $\int_V J_c d\mathbf{v} = 0$ for mass conservation.

Since we are modeling active moving cells which are deformable as well, and may change direction by their own way, we will not require that momentum and energy are conserved during interactions of cells with the ECM or cell-cell interactions. This is the major difference to the theory of Boltzmann equations for diluted gases [6], where mass, momentum and energy are conserved.

Then the transport equation for cell movement is

$$\frac{\partial p}{\partial t} + \mathbf{v} \cdot \nabla_{\mathbf{x}} p + \nabla_{\mathbf{v}} \cdot [\mathbf{f}(\mathcal{C})p] = J_m + J_c. \quad (5)$$

The mathematical theory of Boltzmann equations or kinetic equations in physical context has a long history [4, 6]. In that context, scaling methods and moment closure methods have been developed and the lower order moments have specific physical meanings as particle flux, internal energy, pressure, or energy flux, etc. We believe that these moments play a crucial role for the analysis of transport models in biology. We will introduce the classical moments and adapt the classical notation of pressure and energy, whereby it should be clear that the classical physical interpretation of these terms might not be appropriate. There is, however, a statistical interpretation of these terms, which we will illustrate now.

Adapting the classical notion we denote the cell (number) density by ρ , the population flux (momentum) by $\mathbf{j} = \rho \mathbf{U}$, where \mathbf{U} denotes the mean cell velocity:

$$\rho(t, \mathbf{x}) = \int_V p(t, \mathbf{x}, \mathbf{v}) d\mathbf{v}, \quad (6)$$

$$\rho(t, \mathbf{x}) \mathbf{U}(t, \mathbf{x}) = \int_V p(t, \mathbf{x}, \mathbf{v}) \mathbf{v} d\mathbf{v}. \quad (7)$$

Further we introduce the internal energy E as

$$E(t, \mathbf{x}) = \int_V \frac{1}{2} p(t, \mathbf{x}, \mathbf{v}) |\mathbf{v} - \mathbf{U}(t, \mathbf{x})|^2 d\mathbf{v}. \quad (8)$$

Seen from the statistical point of view, the energy is proportional to the variance in the speed of the cells. We also define a pressure tensor \mathbb{P} and a term corresponding

to an energy flux \mathbf{q} by

$$\mathbb{P}(t, \mathbf{x}) = \int_V p(t, \mathbf{x}, \mathbf{v}) [\mathbf{v} - \mathbf{U}(t, \mathbf{x})] \otimes [\mathbf{v} - \mathbf{U}(t, \mathbf{x})] d\mathbf{v}, \quad (9)$$

$$\mathbf{q}(t, \mathbf{x}) = \int_V \frac{1}{2} p(t, \mathbf{x}, \mathbf{v}) |\mathbf{v} - \mathbf{U}(t, \mathbf{x})|^2 [\mathbf{v} - \mathbf{U}(t, \mathbf{x})] d\mathbf{v}, \quad (10)$$

and observe that $E = \frac{1}{2} \text{tr}(\mathbb{P})$. The matrix \mathbb{P} is also known as the variance-covariance matrix of the velocity distribution $p(t, \mathbf{x}, \mathbf{v})$ while \mathbf{q} corresponds to a third moment of this distribution. We find the identity

$$\int_V p(t, \mathbf{x}, \mathbf{v}) \mathbf{v} \otimes \mathbf{v} d\mathbf{v} = \mathbb{P}(t, \mathbf{x}) + \rho(t, \mathbf{x}) \mathbf{U}(t, \mathbf{x}) \otimes \mathbf{U}(t, \mathbf{x}), \quad (11)$$

and therefore we can write

$$\int_V p(t, \mathbf{x}, \mathbf{v}) \frac{v^2}{2} d\mathbf{v} = E(t, \mathbf{x}) + \frac{1}{2} \rho(t, \mathbf{x}) \mathbf{U}^2(t, \mathbf{x}), \quad (12)$$

where $U = |\mathbf{U}|$ is the mean speed of the cell population.

2. Moment expansions. The aim of this section is to obtain dynamic balance equations for the population density ρ , the flux $\rho \mathbf{U}$, and the energy E , depending on the higher moments \mathbb{P} and \mathbf{q} . Since the interaction terms J_m and J_c in Eq.(5) do not necessarily preserve momentum and energy, we are particularly interested in the corresponding momentum and energy dissipation terms, denoted respectively by \mathbf{j}_m , \mathbf{j}_c , e_m and e_c .

For simplicity, in the following we will drop the (t, \mathbf{x}) dependency of the distribution functions and of the macroscopic variables. Integrating Eq.(5) over the velocity domain V gives

$$\int_V \frac{\partial p}{\partial t} d\mathbf{v} + \int_V \mathbf{v} \cdot \nabla_{\mathbf{x}} p d\mathbf{v} + \int_V \nabla_{\mathbf{v}} \cdot (\mathbf{f}p) d\mathbf{v} = \int_V J_m d\mathbf{v} + \int_V J_c d\mathbf{v}. \quad (13)$$

Now, under the assumption that p vanishes on ∂V , $\int_V \nabla_{\mathbf{v}} \cdot (\mathbf{f}p) d\mathbf{v} = 0$ due to the divergence theorem. On the other hand, thanks to the mass conservation assumptions (A2) and (A3), the r.h.s. of Eq.(13) vanishes and one obtains the mass conservation equation

$$\frac{\partial \rho}{\partial t} + \nabla_{\mathbf{x}} \cdot (\rho \mathbf{U}) = 0. \quad (14)$$

The integration of the transport equation (5) multiplied by \mathbf{v} gives

$$\begin{aligned} \int_V \frac{\partial}{\partial t} (p\mathbf{v}) d\mathbf{v} + \int_V [\mathbf{v} \cdot \nabla_{\mathbf{x}} p] \mathbf{v} d\mathbf{v} + \int_V [\nabla_{\mathbf{v}} \cdot (\mathbf{f}p)] \mathbf{v} d\mathbf{v} \\ = \int_V J_m \mathbf{v} d\mathbf{v} + \int_V J_c \mathbf{v} d\mathbf{v}. \end{aligned} \quad (15)$$

Writing the identity

$$\nabla_{\mathbf{v}} \cdot (\mathbf{v} \otimes \mathbf{f}p) = \mathbf{f}p \cdot [\nabla_{\mathbf{v}} \mathbf{v}] + [\nabla_{\mathbf{v}} \cdot (\mathbf{f}p)] \mathbf{v}, \quad (16)$$

and observing that $\nabla_{\mathbf{v}} \mathbf{v} = \mathbb{I}$, where \mathbb{I} is the identity matrix, one can write

$$[\nabla_{\mathbf{v}} \cdot (\mathbf{f}p)] \mathbf{v} = \nabla_{\mathbf{v}} \cdot (\mathbf{v} \otimes \mathbf{f}p) - \mathbf{f}p. \quad (17)$$

Again because of the divergence theorem, $\int_V \nabla_{\mathbf{v}} \cdot (\mathbf{v} \otimes \mathbf{f}p) d\mathbf{v} = \mathbf{0}$, and since $\mathbf{f} = \mathbf{f}(\mathcal{C})$ then $\int_V \mathbf{f}(\mathcal{C}) p d\mathbf{v} = \rho \mathbf{f}(\mathcal{C})$, so that Eq.(15) can then be written as

$$\frac{\partial}{\partial t} (\rho \mathbf{U}) + \nabla_{\mathbf{x}} \cdot \int_V p \mathbf{v} \otimes \mathbf{v} d\mathbf{v} = \rho \mathbf{f}(\mathcal{C}) + \mathbf{j}_m + \mathbf{j}_c, \quad (18)$$

where

$$\mathbf{j}_m = \int_V J_m \mathbf{v} \, d\mathbf{v}, \quad \text{and} \quad \mathbf{j}_c = \int_V J_c \mathbf{v} \, d\mathbf{v}, \quad (19)$$

are the moment dissipation terms. Finally, the momentum balance equation is obtained recalling the identity (11)

$$\frac{\partial}{\partial t}(\rho \mathbf{U}) + \nabla_{\mathbf{x}} \cdot (\rho \mathbf{U} \otimes \mathbf{U}) = -\nabla_{\mathbf{x}} \cdot \mathbb{P} + \rho \mathbf{f}(\mathcal{C}) + \mathbf{j}_m + \mathbf{j}_c, \quad (20)$$

which may also be rewritten as

$$\rho \left(\frac{\partial \mathbf{U}}{\partial t} + \mathbf{U} \cdot \nabla_{\mathbf{x}} \mathbf{U} \right) = -\nabla_{\mathbf{x}} \cdot \mathbb{P} + \rho \mathbf{f}(\mathcal{C}) + \mathbf{j}_m + \mathbf{j}_c, \quad (21)$$

using the mass balance equation (14).

To derive an equation for the energy balance we multiply Eq.(5) by $\frac{v^2}{2}$ and integrate

$$\begin{aligned} \int_V \frac{\partial}{\partial t} \left(p \frac{v^2}{2} \right) d\mathbf{v} + \int_V [\mathbf{v} \cdot \nabla_{\mathbf{x}} p] \frac{v^2}{2} d\mathbf{v} + \int_V [\nabla_{\mathbf{v}} \cdot (\mathbf{f}p)] \frac{v^2}{2} d\mathbf{v} \\ = \int_V J_m \frac{v^2}{2} d\mathbf{v} + \int_V J_c \frac{v^2}{2} d\mathbf{v}. \end{aligned} \quad (22)$$

The identities (12) and

$$\nabla_{\mathbf{v}} \cdot \left(\mathbf{f}p \frac{v^2}{2} \right) = \mathbf{v} \cdot \mathbf{f}p + [\nabla_{\mathbf{v}} \cdot (\mathbf{f}p)] \frac{v^2}{2}, \quad (23)$$

as well as

$$\mathbf{q} + \mathbb{P}\mathbf{U} = \int_V p \frac{v^2}{2} (\mathbf{v} - \mathbf{U}) \, d\mathbf{v} = \int_V p \frac{v^2}{2} \mathbf{v} \, d\mathbf{v} - \left(E + \frac{1}{2} \rho U^2 \right) \mathbf{U}, \quad (24)$$

allow us to arrive at the energy balance equation

$$\frac{\partial}{\partial t} \left(E + \frac{1}{2} \rho U^2 \right) + \nabla_{\mathbf{x}} \cdot \left[\left(E + \frac{1}{2} \rho U^2 \right) \mathbf{U} + \mathbf{q} + \mathbb{P}\mathbf{U} \right] = \int_V \mathbf{v} \cdot \mathbf{f}p \, d\mathbf{v} + e_m + e_c, \quad (25)$$

where

$$e_m = \int_V J_m \frac{v^2}{2} \, d\mathbf{v}, \quad \text{and} \quad e_c = \int_V J_c \frac{v^2}{2} \, d\mathbf{v}, \quad (26)$$

are related to the energy exchange due to the interactions between cells and the ECM fibres, and among cells themselves. Since $\mathbf{f} = \mathbf{f}(\mathcal{C})$ then

$$\int_V \mathbf{v} \cdot \mathbf{f}p \, d\mathbf{v} = \rho \mathbf{f} \cdot \mathbf{U}, \quad (27)$$

so that one has the first writing of the energy balance equation

$$\frac{\partial}{\partial t} \left(E + \frac{1}{2} \rho U^2 \right) + \nabla_{\mathbf{x}} \cdot \left[\left(E + \frac{1}{2} \rho U^2 \right) \mathbf{U} \right] = -\nabla_{\mathbf{x}} \cdot (\mathbf{q} + \mathbb{P}\mathbf{U}) + \rho \mathbf{f} \cdot \mathbf{U} + e_m + e_c. \quad (28)$$

Using now the momentum balance in addition to the mass balance, one can rewrite this last equation as

$$\frac{\partial E}{\partial t} + \nabla_{\mathbf{x}} \cdot (E\mathbf{U}) = -\nabla_{\mathbf{x}} \cdot \mathbf{q} - \mathbb{P} : \nabla_{\mathbf{x}} \mathbf{U} - (\mathbf{j}_m + \mathbf{j}_c) \cdot \mathbf{U} + e_m + e_c, \quad (29)$$

where we used the notation $\mathbb{A} : \mathbb{B} = \text{tr}(\mathbb{A} \mathbb{B}^{\mathbf{T}})$.

To summarize, we derived equations for mass conservation (14), momentum balance (21) and energy balance (29). Note that the system of equations for $(\rho, \rho \mathbf{U}, E)$

is not closed, since the distribution $p(t, \mathbf{x}, \mathbf{v})$ is used in the pressure tensor \mathbb{P} and in the energy flux \mathbf{q} . Moreover, appropriate collision terms need to be studied to find expressions for the dissipation terms $\mathbf{j}_m, \mathbf{j}_c, e_m$ and e_c .

3. Interaction operators. In the paper by Hillen [21] only cell-ECM interactions were considered while cell-cell interactions were ignored. Here we like to include cell-cell interaction into the model. To do this we use the second simplest approach (the simplest is setting $J_c = 0$), and we assume that interactions are dominated by pair-interactions. Following [5] the general form of the cell-cell interaction term can be written as

$$\begin{aligned}
 J_c &= \int_V \int_V \eta_c(\mathbf{v}', \mathbf{v}'_*) \psi_c((\mathbf{v}', \mathbf{v}'_*) \rightarrow \mathbf{v}) p(\mathbf{v}') p(\mathbf{v}'_*) d\mathbf{v}' d\mathbf{v}'_* \\
 &- \int_V \int_V \eta_c(\mathbf{v}, \mathbf{v}'_*) \psi_c((\mathbf{v}, \mathbf{v}'_*) \rightarrow \mathbf{v}') p(\mathbf{v}) p(\mathbf{v}'_*) d\mathbf{v}' d\mathbf{v}'_*,
 \end{aligned}$$

where the encounter rate $\eta_c(\mathbf{v}', \mathbf{v}'_*)$ denotes the number of encounters per unit volume and unit time between cell pair with velocities \mathbf{v}' and \mathbf{v}'_* and $\psi_c((\mathbf{v}', \mathbf{v}'_*) \rightarrow \mathbf{v})$ denotes the probability of the transition of a cell having the velocity \mathbf{v}' before the encounter to continue its motion with the velocity \mathbf{v} after having interacted with a cell having a velocity \mathbf{v}'_* .

The cell-ECM interactions were studied in [21]. We generalize the approach and write

$$\begin{aligned}
 J_m &= \int_V \int_{S_+^2} \eta_m(\mathbf{v}', \mathbf{n}') \psi_m((\mathbf{v}', \mathbf{n}') \rightarrow \mathbf{v}) p(\mathbf{v}') m(\mathbf{n}') d\mathbf{v}' d\mathbf{n}' \\
 &- \int_V \int_{S_+^2} \eta_m(\mathbf{v}, \mathbf{n}') \psi_m((\mathbf{v}, \mathbf{n}') \rightarrow \mathbf{v}') p(\mathbf{v}) m(\mathbf{n}') d\mathbf{v}' d\mathbf{n}',
 \end{aligned}$$

where $\eta_m(\mathbf{v}', \mathbf{n}')$ is the encounter rate of a cell with velocity \mathbf{v}' with a fibre with orientation $\mathbf{n}' \in S_+^2$ and $\psi_m((\mathbf{v}', \mathbf{n}') \rightarrow \mathbf{v})$ denotes the probability of the transition of a cell having the velocity \mathbf{v}' before the encounter to continue its motion with the velocity \mathbf{v} after having interacted with a fibre oriented along \mathbf{n}' .

Since particles are conserved during interactions, we have the natural conditions

$$\int_V \psi_c((\mathbf{v}', \mathbf{v}'_*) \rightarrow \mathbf{v}) d\mathbf{v} = 1, \quad \text{and} \quad \int_V \psi_m((\mathbf{v}', \mathbf{n}') \rightarrow \mathbf{v}) d\mathbf{v} = 1, \quad (30)$$

so that

$$\begin{aligned}
 J_c &= \int_V \int_V \eta_c(\mathbf{v}', \mathbf{v}'_*) \psi_c((\mathbf{v}', \mathbf{v}'_*) \rightarrow \mathbf{v}) p(\mathbf{v}') p(\mathbf{v}'_*) d\mathbf{v}' d\mathbf{v}'_* \\
 &- p(\mathbf{v}) \int_V \eta_c(\mathbf{v}, \mathbf{v}'_*) p(\mathbf{v}'_*) d\mathbf{v}'_*,
 \end{aligned} \quad (31)$$

and

$$\begin{aligned}
 J_m &= \int_V \int_{S_+^2} \eta_m(\mathbf{v}', \mathbf{n}') \psi_m((\mathbf{v}', \mathbf{n}') \rightarrow \mathbf{v}) p(\mathbf{v}') m(\mathbf{n}') d\mathbf{v}' d\mathbf{n}' \\
 &- p(\mathbf{v}) \int_{S_+^2} \eta_m(\mathbf{v}, \mathbf{n}') m(\mathbf{n}') d\mathbf{n}'.
 \end{aligned} \quad (32)$$

We will use the following hypothesis to simplify the interaction terms. These assumptions are on the one hand realistic for the biological application in mind, on the other hand they enable us to explicitly compute the momentum and energy dissipation terms $\mathbf{j}_c, \mathbf{j}_m, e_c$ and e_m .

- A4:** The encounter rate η_c does not depend on the particular incoming velocities.
A5: The encounter rate η_m does not depend on the particular incoming velocity nor on the fibre orientation.
A6: The transition probability density ψ_c does not depend on the particular incoming velocities, but only on the outgoing velocity modulus.
A7: After the interaction with a fibre oriented along a direction \mathbf{n} cell tends to align with it (i.e., $\hat{\mathbf{v}} = \pm\mathbf{n}$), independently from the particular incoming velocity.

This means that during the interactions, cells have no memory of the velocity they had before the encounter, so that the transition probability densities define the possible range of outgoing velocities regardless of the incoming velocity. Painter [25] currently considers a model without chemotaxis and without cell-cell interactions, but with the inclusion of persistence. Which means cells keep a memory of their past velocities. This is a key ingredient in the formation of vascular networks in vitro [3, 19, 26]. However we will not take it into account, focusing rather on the interactions with the surrounding environment.

Our assumptions (A4) and (A6) allow us to simplify considerably the cell-cell interaction term. Actually the transition probability density ψ_c can be taken as

$$\psi_c((\mathbf{v}', \mathbf{v}'_*) \rightarrow \mathbf{v}) \equiv \psi_c(\mathbf{v}) = \frac{1}{4\pi} \bar{\psi}_c(v), \quad (33)$$

where, keeping in mind condition (30), the function $\bar{\psi}_c(v)$ has to satisfy

$$\int_{\mathbb{R}_+} \bar{\psi}_c(v) v^2 dv = 1. \quad (34)$$

Note that for any distribution $\psi_c(\mathbf{v})$, the cell-cell interaction term becomes

$$\begin{aligned} J_c &= \eta_c \psi_c(\mathbf{v}) \int_V \int_V p(\mathbf{v}') p(\mathbf{v}'_*) d\mathbf{v}' d\mathbf{v}'_* - \eta_c p(\mathbf{v}) \int_V p(\mathbf{v}'_*) d\mathbf{v}'_* \\ &= \eta_c \rho [\rho \psi_c(\mathbf{v}) - p(\mathbf{v})], \end{aligned} \quad (35)$$

which satisfies

$$\int_V J_c d\mathbf{v} = \eta_c \rho \int_V [\rho \psi_c(\mathbf{v}) - p(\mathbf{v})] d\mathbf{v} = 0, \quad (36)$$

corresponding to mass conservation during cell-cell interaction.

In order to compute the higher moments of J_c it is useful to observe that due to the specific dependency (33) of ψ_c on the velocity modulus, we have

$$\int_V \psi_c(\mathbf{v}) \mathbf{v} d\mathbf{v} = \mathbf{0}. \quad (37)$$

For the same reason, the following tensor is diagonal,

$$\int_V \psi_c(\mathbf{v}) \mathbf{v} \otimes \mathbf{v} d\mathbf{v} = \sigma_c \mathbb{I}, \quad (38)$$

where we defined the variance σ_c as

$$\sigma_c = \frac{1}{3} \int_{\mathbb{R}_+} \bar{\psi}_c(v) v^4 dv. \quad (39)$$

From this variance, it is possible to define the order of magnitude of the characteristic mesenchymal velocity. To be more specific, if all cells move with the same speed U_c then $\sigma_c = U_c^2/3$.

One can then explicitly compute \mathbf{j}_c and e_c as

$$\begin{aligned}\mathbf{j}_c &= \int_V J_c \mathbf{v} \, d\mathbf{v} = \eta_c \rho \int_V [\rho \psi_c(\mathbf{v}) \mathbf{v} - p(\mathbf{v}) \mathbf{v}] \, d\mathbf{v} \\ &= -\eta_c \rho^2 \mathbf{U},\end{aligned}\quad (40)$$

and

$$\begin{aligned}e_c &= \int_V J_c \frac{v^2}{2} \, d\mathbf{v} = \eta_c \rho \int_V \left[\rho \psi_c(\mathbf{v}) \frac{v^2}{2} - p(\mathbf{v}) \frac{v^2}{2} \right] \, d\mathbf{v} \\ &= \eta_c \rho \left[\frac{3}{2} \rho \sigma_c - \left(E + \frac{1}{2} \rho U^2 \right) \right].\end{aligned}\quad (41)$$

We will proceed in a similar way for the interaction with the fibres of the ECM. The independency from the incoming velocity, i.e. assumptions (A5) and (A7), allows us to reduce the expression (32) to

$$J_m = \eta_m \left[\rho \int_{S^2_+} \psi_m((\mathbf{v}', \mathbf{n}') \rightarrow \mathbf{v}) m(\mathbf{n}') \, d\mathbf{n}' - Mp(\mathbf{v}) \right]. \quad (42)$$

In addition, the assumption that after the interaction with a fibre cell tends to align with it allows us to take as a transition probability density the function

$$\psi_m((\mathbf{v}', \mathbf{n}') \rightarrow \mathbf{v}) \equiv \psi_m(\mathbf{n}'; \mathbf{v}) = \psi_m(v) \frac{1}{2} [\delta(\mathbf{n}' - \hat{\mathbf{v}}) + \delta(\mathbf{n}' + \hat{\mathbf{v}})], \quad (43)$$

where the δ 's are Dirac deltas and (see condition (30)) $\psi_m(v)$ has to satisfy

$$\int_{\mathbb{R}_+} \psi_m(v) v^2 \, dv = 1. \quad (44)$$

Hence,

$$J_m = \begin{cases} \frac{\eta_m}{2} \rho \psi_m(v) m(\hat{\mathbf{v}}) - \eta_m Mp(\mathbf{v}) & \text{for } \hat{\mathbf{v}} \in S^2_+, \\ \frac{\eta_m}{2} \rho \psi_m(v) m(-\hat{\mathbf{v}}) - \eta_m Mp(\mathbf{v}) & \text{for } \hat{\mathbf{v}} \in S^2_-, \end{cases} \quad (45)$$

and using m^e as extended over S^2 by symmetry leads to

$$J_m = \eta_m \left[\frac{1}{2} \rho \psi_m(v) m^e(\hat{\mathbf{v}}) - Mp(\mathbf{v}) \right]. \quad (46)$$

It is trivial to check that for any distribution $\psi_m(v)$

$$\int_V J_m \, d\mathbf{v} = \eta_m \rho \left[\int_{\mathbb{R}_+} \psi_m(v) v^2 \, dv \cdot \frac{1}{2} \int_{S^2} m^e(\hat{\mathbf{v}}) \, d\hat{\mathbf{v}} - M \right] = 0, \quad (47)$$

corresponding to mass conservation during cell-ECM interaction.

On the other hand, thanks to the symmetry property (3), one has that

$$\begin{aligned}\mathbf{j}_m &= \int_V J_m \mathbf{v} \, d\mathbf{v} \\ &= \eta_m \left[\frac{1}{2} \rho \int_{\mathbb{R}_+} \psi_m(v) v^3 \, dv \cdot \int_{S^2} m^e(\hat{\mathbf{v}}) \hat{\mathbf{v}} \, d\hat{\mathbf{v}} - M \rho \mathbf{U} \right] \\ &= -\eta_m M \rho \mathbf{U},\end{aligned}\quad (48)$$

and

$$\begin{aligned}
e_m &= \int_V J_m \frac{v^2}{2} d\mathbf{v} \\
&= \eta_m \left[\frac{1}{2} \rho \int_{\mathbb{R}_+} \psi_m(v) v^4 dv \cdot \frac{1}{2} \int_{S^2} m^e(\hat{\mathbf{v}}) d\hat{\mathbf{v}} - M \int_V p(\mathbf{v}) \frac{v^2}{2} d\mathbf{v} \right] \\
&= \eta_m M \left[\frac{3}{2} \rho \sigma_m - \left(E + \frac{1}{2} \rho U^2 \right) \right],
\end{aligned} \tag{49}$$

where the variance

$$\sigma_m = \frac{1}{3} \int_{\mathbb{R}_+} \psi_m(v) v^4 dv, \tag{50}$$

is introduced for the cell-ECM interactions in the same way as for the cell-cell interactions.

The planar case ($\mathbf{v} \in V \subseteq \mathbb{R}^2$ and $\mathbf{n} \in S_+^1$) can be deduced in a similar way (see [8]).

With the specific interaction operators (35) and (46) the general transport equation becomes

$$\begin{aligned}
\frac{\partial p}{\partial t} + \mathbf{v} \cdot \nabla_{\mathbf{x}} p + \nabla_{\mathbf{v}} \cdot (\mathbf{f} p) &= \eta_c \rho [\rho \psi_c(\mathbf{v}) - p(\mathbf{v})] \\
&+ \eta_m \left[\frac{1}{2} \rho \psi_m(v) m^e(\hat{\mathbf{v}}) - M p(\mathbf{v}) \right].
\end{aligned} \tag{51}$$

Finally, expressions (40) and (48) of the moment dissipations \mathbf{j}_c and \mathbf{j}_m allow us to write the momentum balance equation (21) as

$$\rho \left(\frac{\partial \mathbf{U}}{\partial t} + \mathbf{U} \cdot \nabla_{\mathbf{x}} \mathbf{U} \right) = -\nabla_{\mathbf{x}} \cdot \mathbb{P} + \rho \mathbf{f}(\mathcal{C}) - (\eta_m M + \eta_c \rho) \rho \mathbf{U}, \tag{52}$$

where the last term can be identified as the drag forces due to the cell interactions with the ECM and the other cells. With regard to the energy balance equation, Eq.(28) can be rewritten as

$$\begin{aligned}
\frac{\partial}{\partial t} \left(E + \frac{1}{2} \rho U^2 \right) + \nabla_{\mathbf{x}} \cdot \left[\left(E + \frac{1}{2} \rho U^2 \right) \mathbf{U} \right] &= -\nabla_{\mathbf{x}} \cdot (\mathbf{q} + \mathbb{P} \mathbf{U}) + \rho \mathbf{f} \cdot \mathbf{U} \\
&+ \frac{3}{2} \rho (\eta_m \sigma_m M + \eta_c \sigma_c \rho) - (\eta_m M + \eta_c \rho) \left(E + \frac{1}{2} \rho U^2 \right),
\end{aligned} \tag{53}$$

by using the expressions (41) and (49) of the energy dissipations e_c and e_m . The last term is an energy dissipation due to the drag forces acting on the cells, while the previous term is an energy production term related to the fact that cells tend to move with a characteristic mesenchymal velocity achievable through internal metabolic processes (i.e. internal energy production) not considered here in detail.

Of course, the system of equations (14), (52) and (53) is still not closed, since the pressure tensor \mathbb{P} and the energy flux \mathbf{q} depend on the full distribution $p(t, \mathbf{x}, \mathbf{v})$. However, the transport equation (51) is by itself of the greatest interest. Actually, simple kinetic models of reorientation have already exhibited interesting results with regard to pattern formation as in [20], and we believe that the numerical study of Eq.(51) will give rise to new and very original results.

One possibility to close the macroscopic system is to evaluate \mathbb{P} and \mathbf{q} at the statistical equilibrium, as it will be proposed in Section 5. However, using this closure, it is not obvious that the solution of the macroscopic system is an approximation of

the moments of the solution p of Eq.(51). The other possibility consists of using formal asymptotic methods that require the existence of a small parameter ε for scaling processes. The Chapman-Enskog expansion requires a number of macroscopic unknowns directly related to the number of invariants of the interaction operators. So in the following section we propose to approximate the solution p of Eq.(51) using the Hilbert expansion. At this stage, due to the fact that only mass is preserved in our model, we chose to perform a diffusion limit that has shown to give a good approximation limit to the long time dynamics [22] of the kinetic model under the assumptions used, mainly the existence of the parameter ε . Indeed, connections between hyperbolic and parabolic chemotactic models have been shown in [15] with regards to the stationary solutions. It is worth keeping in mind that this implies, of course, that initial transients can be very different.

4. Diffusion limit. We are interested in this section in the formal diffusion limit of the problem (see [22] for example), i.e. the long time behavior for this strongly collisional system. From a strictly mathematical point of view, rigorous proofs regarding the diffusive limit procedure may be found in [1, 7] for samples of chemotactic models. Introducing the parabolic scaling $\tau = \varepsilon^2 t$, $\xi = \varepsilon \mathbf{x}$ and $\mathbf{f} = \varepsilon \hat{\mathbf{f}}$, where ε is a small dimensionless parameter, allows us to write the transport equation (51) as

$$\varepsilon^2 \frac{\partial p}{\partial \tau} + \varepsilon \nabla_{\xi} \cdot (p \mathbf{v}) + \varepsilon \nabla_{\mathbf{v}} \cdot (\hat{\mathbf{f}} p) = J_m + J_c, \tag{54}$$

where J_m and J_c are the operators particularized in the last section.

We seek the solution of this transport equation under the Hilbert expansion $p_{\varepsilon} = p_0 + \varepsilon p_1 + \mathcal{O}(\varepsilon^2)$. Substituting p_{ε} in equation (54) gives rise to the following cascade of equations

$$\begin{aligned} \varepsilon^0 : \\ 0 = \eta_m \left[\frac{1}{2} \rho_0 \psi_m(v) m^e(\hat{\mathbf{v}}) - M p_0(\mathbf{v}) \right] + \eta_c \rho_0 \left[\rho_0 \psi_c(\mathbf{v}) - p_0(\mathbf{v}) \right], \end{aligned} \tag{55}$$

at the zero-th order, and

$$\begin{aligned} \varepsilon^1 : \\ \nabla_{\xi} \cdot [p_0(\mathbf{v}) \mathbf{v}] + \nabla_{\mathbf{v}} \cdot [\hat{\mathbf{f}} p_0(\mathbf{v})] = \eta_m \left[\frac{1}{2} \rho_1 \psi_m(v) m^e(\hat{\mathbf{v}}) - M p_1(\mathbf{v}) \right] \\ + \eta_c \left[\rho_1 (2 \rho_0 \psi_c(\mathbf{v}) - p_0(\mathbf{v})) - \rho_0 p_1(\mathbf{v}) \right], \end{aligned} \tag{56}$$

at the first order, where for $i = 1, 2$ we noted

$$\rho_i = \int_V p_i(\mathbf{v}) d\mathbf{v}. \tag{57}$$

The zero-th order equation is solved by the equilibrium solution corresponding to $J_m + J_c = 0$, e.g.

$$p_0(\mathbf{v}) = \frac{\rho_0}{\eta_m M + \eta_c \rho_0} \left[\frac{1}{2} \eta_m \psi_m(v) m^e(\hat{\mathbf{v}}) + \eta_c \rho_0 \psi_c(\mathbf{v}) \right]. \tag{58}$$

The first moment of the distribution p_0 is evaluated, using the property (3) due to the fact that m^e is an even function of its argument, as well as the property (37)

related to the random motion of cells. That simply leads to

$$\int_V p_0(\mathbf{v}) \mathbf{v} \, d\mathbf{v} = \mathbf{0}. \quad (59)$$

The solution of the first order equation can also be explicitly calculated from Eq.(56) and is

$$p_1(\mathbf{v}) = \frac{1}{\eta_m M + \eta_c \rho_0} \left[-\nabla_\xi \cdot [p_0(\mathbf{v})\mathbf{v}] - \nabla_{\mathbf{v}} \cdot [\hat{\mathbf{f}}p_0(\mathbf{v})] \right. \\ \left. + \rho_1 \left(\frac{\eta_m}{2} \psi_m(v) m^e(\hat{\mathbf{v}}) + \eta_c (2\rho_0 \psi_c(\mathbf{v}) - p_0(\mathbf{v})) \right) \right]. \quad (60)$$

In the evaluation of the first moment of the distribution p_1 , it is easy to check that the contribution due to the terms appearing in the second line of Eq.(60) vanishes, thanks to the properties (3) and (37), as well as the relation (59), so that this moment becomes simply

$$\int_V p_1(\mathbf{v}) \mathbf{v} \, d\mathbf{v} = \frac{1}{\eta_m M + \eta_c \rho_0} \left[-\int_V \left(\nabla_\xi \cdot [p_0(\mathbf{v})\mathbf{v}] \right) \mathbf{v} \, d\mathbf{v} \right. \\ \left. - \int_V \left(\nabla_{\mathbf{v}} \cdot [\hat{\mathbf{f}}p_0(\mathbf{v})] \right) \mathbf{v} \, d\mathbf{v} \right]. \quad (61)$$

Applying the identity (17) to the distribution function p_0 and following the method used to obtain Eq.(18) in Section 2 allows us to write this moment as

$$\int_V p_1(\mathbf{v}) \mathbf{v} \, d\mathbf{v} = \frac{1}{\eta_m M + \eta_c \rho_0} \left[-\nabla_\xi \cdot \int_V p_0(\mathbf{v}) \mathbf{v} \otimes \mathbf{v} \, d\mathbf{v} + \rho_0 \hat{\mathbf{f}} \right]. \quad (62)$$

Notice that the integral term in the r.h.s. is simply the pressure tensor taken at the equilibrium.

We now derive the evolution equation for the approximation ρ_ε of the cell number density. This quantity is defined by

$$\rho_\varepsilon = \int_V p_\varepsilon(\mathbf{v}) \, d\mathbf{v}, \quad (63)$$

and can be expanded in

$$\rho_\varepsilon = \rho_0 + \varepsilon \rho_1 + \mathcal{O}(\varepsilon^2). \quad (64)$$

Starting again from the transport equation (54), multiplied by ε^{-2} and integrated over the velocity domain V leads to

$$\int_V \frac{\partial p_\varepsilon(\mathbf{v})}{\partial \tau} \, d\mathbf{v} + \frac{1}{\varepsilon} \nabla_\xi \cdot \int_V p_\varepsilon(\mathbf{v}) \mathbf{v} \, d\mathbf{v} + \frac{1}{\varepsilon} \int_V \nabla_{\mathbf{v}} \cdot [\hat{\mathbf{f}}p_\varepsilon(\mathbf{v})] \, d\mathbf{v} \\ = \frac{1}{\varepsilon^2} \int_V J_m \, d\mathbf{v} + \frac{1}{\varepsilon^2} \int_V J_c \, d\mathbf{v}. \quad (65)$$

Now under the assumption that p_ε vanishes on the boundary ∂V , the last integral on the l.h.s. vanishes due to the divergence theorem, while the r.h.s. vanishes due to the mass conservation assumption. Hence one obtains the mass balance equation

$$\frac{\partial \rho_\varepsilon}{\partial \tau} + \frac{1}{\varepsilon} \nabla_\xi \cdot \int_V p_\varepsilon(\mathbf{v}) \mathbf{v} \, d\mathbf{v} = 0. \quad (66)$$

Injecting the expansion (64), and keeping in mind the relation (59), gives at the main order

$$\frac{\partial \rho_0}{\partial \tau} + \nabla_\xi \cdot \int_V p_1(\mathbf{v}) \mathbf{v} \, d\mathbf{v} = 0, \quad (67)$$

that leads finally, substituting Eq.(62), to the final equation for the zero-th order of approximation of the cell number density:

$$\frac{\partial \rho_0}{\partial \tau} = \nabla_{\xi} \cdot \left[\frac{\nabla_{\xi} \cdot \mathbb{P}_0 - \rho_0 \hat{\mathbf{f}}}{\eta_m M + \eta_c \rho_0} \right], \tag{68}$$

where

$$\mathbb{P}_0 = \int_V p_0(\mathbf{v}) \mathbf{v} \otimes \mathbf{v} d\mathbf{v}, \tag{69}$$

denotes the pressure tensor at the equilibrium.

5. Closure through the equilibrium distribution. The aim of this section is to determine the mean quantities at the equilibrium. It will be a way to close the different approaches of the last two sections, while keeping in mind the loss of information due to this limiting procedure.

First note that the zero-th order momentum $\mathbf{j}_0 = \rho_0 \mathbf{U}_0$ has already been computed (see Eq.(59)) and leads to a null mean velocity

$$\mathbf{U}_0 = \frac{1}{\rho_0} \int_V p_0(\mathbf{v}) \mathbf{v} d\mathbf{v} = \mathbf{0}. \tag{70}$$

So the next step consists in calculating the pressure tensor \mathbb{P}_0 at the equilibrium. Using the expression (58) of the distribution function p_0 leads us to split this calculus into two parts. The first one corresponds to a pressure term due to the cell-ECM interactions while the second one is related to cell-cell interactions. Recalling the definitions (4) of the orientation tensor \mathbb{D} , as well as the variance σ_m (respectively σ_c) defined by (50) (respectively by (39)) leads to the explicit expression

$$\mathbb{P}_0 = \frac{\rho_0}{\eta_m M + \eta_c \rho_0} (\eta_m \sigma_m M \mathbb{D} + \eta_c \sigma_c \rho_0 \mathbb{I}). \tag{71}$$

In particular, if $\sigma_m = \sigma_c \equiv \sigma$, corresponding to an equivalent post-interaction random speed for each type of encounter, we have

$$\mathbb{P}_0 = \sigma \rho_0 \mathbb{I} + \frac{\eta_m \sigma M}{\eta_m M + \eta_c \rho_0} (\mathbb{D} - \mathbb{I}) \rho_0. \tag{72}$$

For completeness, we remark that evaluating the heat flux $\mathbf{q} \equiv \mathbf{q}_0$ for the equilibrium distribution gives

$$\mathbf{q}_0 = \int_V p_0(\mathbf{v}) \frac{1}{2} v^2 \mathbf{v} d\mathbf{v} = \mathbf{0}. \tag{73}$$

Taking the specific structure $\mathbf{f}(\mathcal{C}) = \lambda \nabla_{\mathbf{x}} \mathcal{C}$ of the chemotactic force proposed in the assumption (A1), we are capable to write the continuum equation for the evolution of the cell density zero-th order approximation. For simplicity in the notation, we drop out the subscript related to the order of approximation so that, in the usual variables t and \mathbf{x} , one has

$$\begin{aligned} \frac{\partial \rho}{\partial t} + \nabla_{\mathbf{x}} \cdot \left(\frac{\lambda \rho \nabla_{\mathbf{x}} \mathcal{C}}{\eta_m M + \eta_c \rho} \right) &= \nabla_{\mathbf{x}} \cdot \left[\frac{\nabla_{\mathbf{x}}(\sigma \rho)}{\eta_m M + \eta_c \rho} \right] \\ &+ \nabla_{\mathbf{x}} \cdot \left[\frac{1}{\eta_m M + \eta_c \rho} \nabla_{\mathbf{x}} \cdot \left(\frac{\eta_m \sigma M}{\eta_m M + \eta_c \rho} (\mathbb{D} - \mathbb{I}) \rho \right) \right]. \end{aligned} \tag{74}$$

The first term on the r.h.s gives rise to an isotropic diffusion term, while the second one takes into account possible anisotropies due to the presence of the fibrous network.

6. ECM remodeling. In the present section, we want to include the proteolytic activity of moving cells to open their way through the ECM proposing the following model for the evolution of the fibrous network

$$\frac{\partial m}{\partial t}(t, \mathbf{x}, \mathbf{n}) = -\mathcal{L}_m(p(t, \mathbf{x}, \mathbf{v}), \mathbf{n}) (m(t, \mathbf{x}, \mathbf{n}) - m_0(t, \mathbf{x}, \mathbf{n})), \quad (75)$$

where m_0 takes into account the possibility that only some constituents of the ECM are degraded by the proteolytic activity of the cells, e.g. the ECM collagen fibres, and not others so that even if all collagen fibres are locally degraded, there is no vacuum in the ECM.

We model the degradation term \mathcal{L}_m by the following Boltzmann-like interaction term

$$\mathcal{L}_m \equiv \mathcal{L}_m(t, \mathbf{x}, \mathbf{n}) = \int_V \eta_m K(\mathbf{v}, \mathbf{n}) p(t, \mathbf{x}, \mathbf{v}) d\mathbf{v}, \quad (76)$$

where $K(\mathbf{v}, \mathbf{n})$ is the fibre degradation rate. We assume that the proteolytic kernel K only depends on the angle between the direction of the fibre and the cell trajectory, so that it vanishes when the cell is aligned with the fibre and has maximum activity if cell motion is orthogonal to the fibre, e.g. $K(\mathbf{v}, \mathbf{n}) \equiv \bar{K}(|\hat{\mathbf{v}} \cdot \mathbf{n}|)$. As introduced in [21], the system consisting of the cell transport equation (51) and the fibre network equation (75), where the degradation term is modeled by (76), is called *transport model for mesenchymal motion*.

Evaluating the integral in (76) using the equilibrium distribution (58), coherently with the expansion introduced in Section 4, we can write

$$\begin{aligned} \int_V \bar{K}(|\hat{\mathbf{v}} \cdot \mathbf{n}|) p_0(\mathbf{v}) d\mathbf{v} &= \frac{\rho_0}{\eta_m M + \eta_c \rho_0} \int_V \bar{K}(|\hat{\mathbf{v}} \cdot \mathbf{n}|) \cdot \\ &\quad \left[\frac{\eta_m}{2} \psi_m(v) m^e(\hat{\mathbf{v}}) + \eta_c \rho_0 \psi_c(\mathbf{v}) \right] d\mathbf{v} \\ &= \frac{\rho_0}{\eta_m M + \eta_c \rho_0} \left[\frac{\eta_m}{2} \int_{S^2} \bar{K}(|\hat{\mathbf{v}} \cdot \mathbf{n}|) m^e(\hat{\mathbf{v}}) d\hat{\mathbf{v}} \right. \\ &\quad \left. + \frac{\eta_c \rho_0}{4\pi} \int_{S^2} \bar{K}(|\hat{\mathbf{v}} \cdot \mathbf{n}|) d\hat{\mathbf{v}} \right]. \end{aligned} \quad (77)$$

Hence, dropping out the subscript zero as well as the (t, \mathbf{x}) dependency, Eq.(75) rewrites

$$\frac{\partial m}{\partial t}(\mathbf{n}) = -\eta_m \rho \left[\frac{\eta_m \chi(m^e, \mathbf{n}) M + \eta_c \mathcal{K} \rho}{\eta_m M + \eta_c \rho} \right] (m(\mathbf{n}) - m_0(\mathbf{n})), \quad (78)$$

where

$$\chi(m^e, \mathbf{n}) = \frac{1}{2M} \int_{S^2} \bar{K}(|\hat{\mathbf{v}} \cdot \mathbf{n}|) m^e(\hat{\mathbf{v}}) d\hat{\mathbf{v}}, \quad (79)$$

and

$$\mathcal{K} = \frac{1}{4\pi} \int_{S^2} \bar{K}(|\hat{\mathbf{v}} \cdot \mathbf{n}|) d\hat{\mathbf{v}}, \quad (80)$$

is a constant which, due to the symmetry argument, does not depend on \mathbf{n} . Equation (78) can be coupled to Eq.(74) to include ECM remodeling.

It can be observed that since the minimum of \bar{K} is obtained when $\hat{\mathbf{v}}$ and \mathbf{n} are parallel, then the minimum of the function χ can be expected when \mathbf{n} corresponds to the maximum of m^e , that is the minimum degradation is obtained along the main direction of the fibres, and viceversa, the maximum degradation should be expected for orthogonal directions.

To be specific, if $\bar{K}(|\hat{\mathbf{v}} \cdot \mathbf{n}|) = \mu(1 - |\hat{\mathbf{v}} \cdot \mathbf{n}|^\beta)$ for $\mu \in [0, 1]$ and $\beta \geq 0$, then one has

$$\chi \equiv \mu \left(1 - \frac{\int_{S^2} |\hat{\mathbf{v}} \cdot \mathbf{n}|^\beta m^e(\hat{\mathbf{v}}) d\hat{\mathbf{v}}}{\int_{S^2} m^e(\hat{\mathbf{v}}) d\hat{\mathbf{v}}} \right) \quad \text{and} \quad \mathcal{K} \equiv \frac{\mu\beta}{1 + \beta}. \quad (81)$$

Then the evolution of the fibres with orientation $\mathbf{n} \in S_+^2$ is given by

$$\frac{\partial m}{\partial t}(\mathbf{n}) = -\mathcal{L}_m(\mathbf{n})(m(\mathbf{n}) - m_0(\mathbf{n})), \quad (82)$$

where

$$\mathcal{L}_m(\mathbf{n}) = \frac{\eta_m \mu \rho}{\eta_m M + \eta_c \rho} \left[\frac{\eta_m}{2} \int_{S^2} (1 - |\hat{\mathbf{v}} \cdot \mathbf{n}|^\beta) m^e(\hat{\mathbf{v}}) d\hat{\mathbf{v}} + \frac{\eta_c \beta \rho}{1 + \beta} \right]. \quad (83)$$

7. Numerical simulations. We present in this section numerical simulations in order to emphasize the ability of the model to describe interesting behaviors related to cell motion in the ECM. More precisely, we will show how the motion is influenced either by the inhomogeneity or by the anisotropy of a stationary distribution of fibres. To this aim, we do not consider the proteolytic activity of moving cells, as proposed in the previous section, and we deal with the cell motion equation (74) only. The description of the ECM is then given once and for all in each numerical experiment. Simulations performed at the kinetic level, including ECM remodeling, but without cell-cell interactions and without chemotaxis can be found in Painter [25], while the numerical study of the transport equation (51) will be presented in a future work.

So we are dealing with the following mass transport equation which has been rewritten in a more compact way as

$$\frac{\partial \rho}{\partial t} + \nabla_{\mathbf{x}} \cdot \left[\frac{\rho \mathbf{f}(\mathcal{C})}{\eta_m M + \eta_c \rho} \right] = \nabla_{\mathbf{x}} \cdot \left[\frac{1}{\eta_m M + \eta_c \rho} \nabla_{\mathbf{x}} \cdot \left(\frac{\sigma \rho (\eta_m M \mathbb{D} + \eta_c \rho \mathbb{I})}{\eta_m M + \eta_c \rho} \right) \right], \quad (84)$$

where the cell number density has been normalized by the constant number of cells in the domain \mathcal{D} , so that

$$\int_{\mathcal{D}} \rho(t, \mathbf{x}) d\mathbf{x} = \int_{\mathcal{D}} \rho(t = 0, \mathbf{x}) d\mathbf{x} = 1. \quad (85)$$

The stationary fibre density has also been normalized, with respect to the total number of fibres in the domain so that

$$\int_{\mathcal{D}} M(\mathbf{x}) d\mathbf{x} = 1. \quad (86)$$

In a first approach and for visualization facility reason, we will consider the two-dimensional case and we derive the dimensionless equation for cell motion in this particular case. To this aim, we introduce the normalized $\tilde{\cdot}$ -quantities:

- Distances are scaled by a physical (or biological) length L related either to an experimental setup or to an in vivo phenomenon, so that $\mathbf{x} = L\tilde{\mathbf{x}}$ and the domain \mathcal{D} reduces to $[0, 1] \times [0, 1]$;
- Times are scaled by a time T so that $t = T\tilde{t}$;
- External forces are scaled by a given intensity F so that $\mathbf{f} = F\tilde{\mathbf{f}}$.

Substituting this new system of variables into Eq.(84) leads to

$$\frac{1}{T} \frac{\partial \rho}{\partial \tilde{t}} + \frac{F}{\eta_m L} \nabla_{\tilde{\mathbf{x}}} \cdot \left[\frac{\rho \tilde{\mathbf{f}}(\mathcal{C})}{M + \alpha \rho} \right] = \frac{\sigma}{\eta_m L^2} \nabla_{\tilde{\mathbf{x}}} \cdot \left[\frac{1}{M + \alpha \rho} \nabla_{\tilde{\mathbf{x}}} \cdot \left(\frac{\rho (M \mathbb{D} + \alpha \rho \mathbb{I})}{M + \alpha \rho} \right) \right], \quad (87)$$

where $\nabla_{\tilde{\mathbf{x}}} \cdot (\cdot)$ denotes the L -normalized divergence operator and $\alpha = \eta_c/\eta_m$. Thus scaling time by $T = \eta_m L^2/\sigma$ gives the dimensionless equation

$$\frac{\partial \rho}{\partial \tilde{t}} + \mathcal{P}_e \nabla_{\tilde{\mathbf{x}}} \cdot \left[\frac{\rho \tilde{\mathbf{f}}(\mathcal{C})}{M + \alpha \rho} \right] = \nabla_{\tilde{\mathbf{x}}} \cdot \left[\frac{1}{M + \alpha \rho} \nabla_{\tilde{\mathbf{x}}} \cdot \left(\frac{\rho(M\mathbb{D} + \alpha\rho\mathbb{I})}{M + \alpha\rho} \right) \right], \quad (88)$$

where $\mathcal{P}_e = FL/\sigma$ is a dimensionless Peclet number written according to the physical parameters of the problem, that compares the influence on motion of the taxis (advection) with respect to the random walk/contact guidance (diffusion). Thus $\mathcal{P}_e \gg 1$ when advection is dominant, while on the contrary $\mathcal{P}_e \ll 1$ for diffusion-dominated motion. With regard to the parameter α , it is a way to compare the diffusion-like motions induced either by cell-cell or by cell-ECM interactions.

As a conclusion, once the stationary fibre distribution m^e is given, the density M as well as the tensor \mathbb{D} can be evaluated once and for all, so that the problem depends only on the two parameters \mathcal{P}_e and α .

We propose two series of simulations. The first one consists in putting a gaussian-like concentration of a chemorepellent substance at the center of the domain. We show in different cases (however here always isotropic, i.e. $\mathbb{D} = \mathbb{I}$) how the solution accounts for inhomogeneities either of the ECM or of the initial distribution of cells. We also show for each case how the solution tends to a stationary axi-symmetric configuration.

The second set of simulations account for motion induced by a constant chemoattractive force. We will show how both inhomogeneities and anisotropy of the ECM affect the motion.

So we consider the first configuration where the chemotactic force is radial and given by $\mathbf{f} = f(r)\mathbf{e}_r$ where the intensity f is shown in Fig.1. The values of the two parameters of the model are chosen as $\mathcal{P}_e = 50$ and $\alpha = 1$, and they will remain the same in all the cases presented in Fig.3.

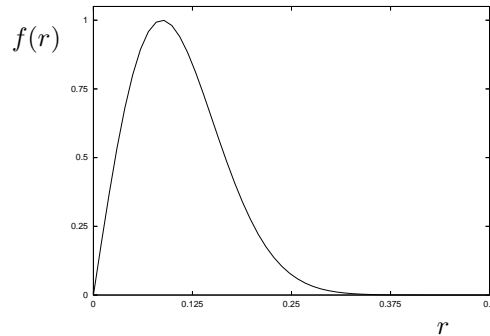


FIGURE 1. Dimensionless radial chemorepellent force induced by a gaussian-like distribution of chemical substance. The radius r corresponds to the distance from the center $x = 0.5$ and $y = 0.5$ of the domain $\mathcal{D} = [0, 1] \times [0, 1]$.

The left column of Fig.3 shows the evolution of the cell density in an homogeneous set of fibres $M(\mathbf{x}) = \text{Constant}$. Due to the radial expression of the force \mathbf{f} , and starting from a constant initial distribution of cells, cells tend to move away from the

chemical substance in an axi-symmetric way. A circular “hole” appears in the cell density, centered at the mean position of the chemorepellent, and surrounded by an accumulation (higher density) of cells where the intensity of the chemorepellent force begins to decrease significantly. In a second step, when this hole is stabilized, the cell accumulation ring tends to homogenize itself due to the random-walk motion of the cells. The solution reaches a stationary state that can be computed analytically as proposed in the one-dimensional case in [8]. The numerical stationary solution is compared to the analytical one in Figure 4.

In the central column of Fig.3, possible inhomogeneity of the fibrous network is taken into account, introducing a particular space-varying fibre density represented in Fig.2. Starting again from a constant initial distribution of cells, the motion is slowed down where high density of fibre takes place.

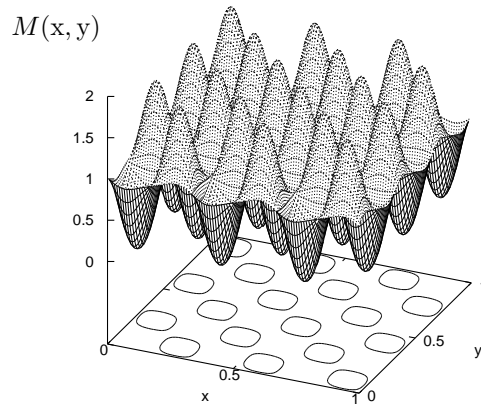
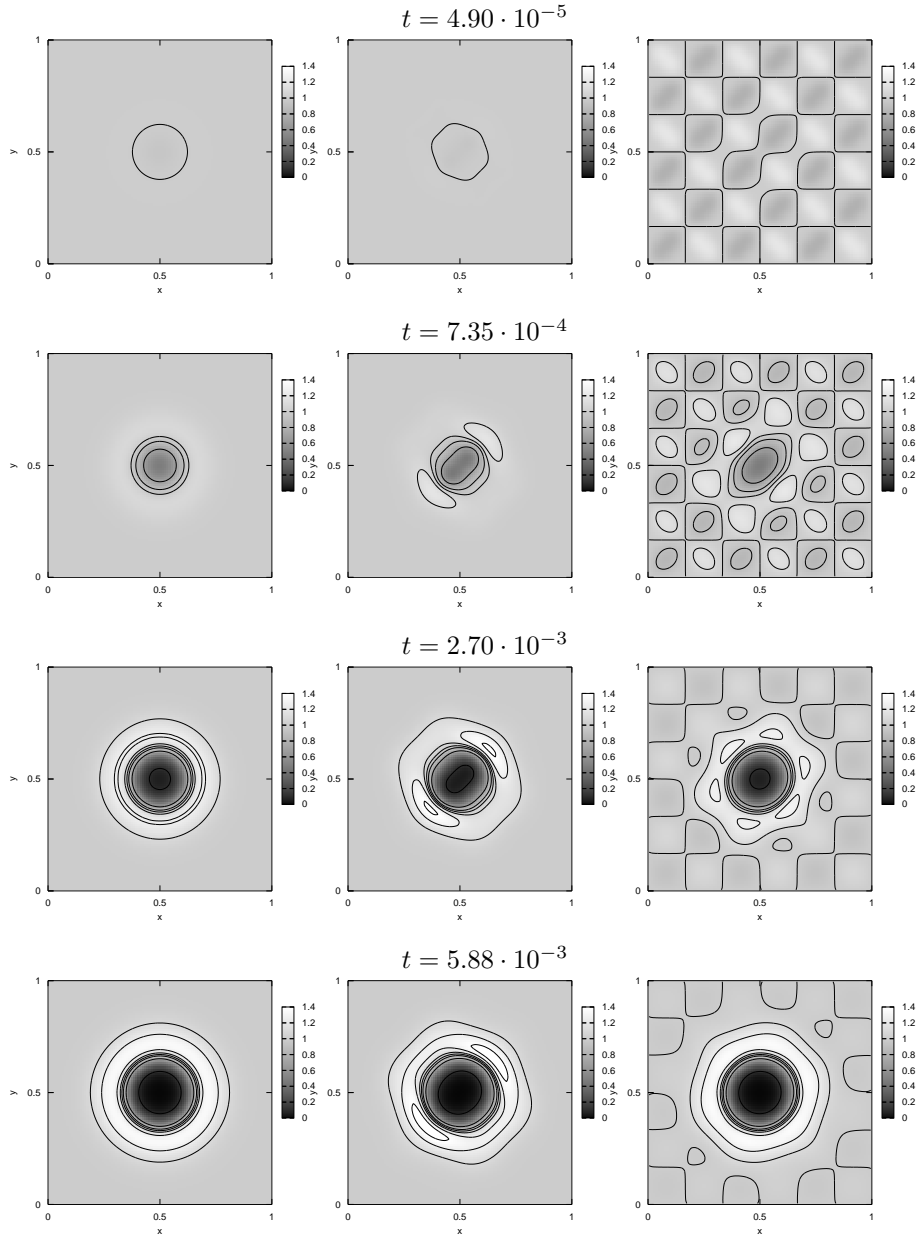


FIGURE 2. Oscillatory distribution of the fibre density corresponding to the simulation shown in the central column of the Figure 3. Shapes plotted at the bottom show locations of high density.

So the axi-symmetry of the evolution is lost and one can observe a quicker development of the hole where fibres are less dense. More precisely, the hole appears in an elongated shape whose axis is given by two low fibre density locations (see Fig.2). At the extremities of this axis, two areas of high density are observed. In a second step, when the hole is about to be stabilized, the two cell accumulation areas tend to homogenize themselves in the same way as in the axi-symmetric case to lead finally to the same stationary state as previously.

To finish, in the right column of Figure 3 we consider an inhomogeneous initial distribution of cells, cells which are about to move through an homogeneous fibre network $M(\mathbf{x}) = \text{Constant}$. Two phenomena take place as soon as the motion begins: if far enough from the repellent field, high (respectively low) density locations tend to decrease (respectively increase) due to the random-walk motion of the cells. On the other hand, the hole formation triggered by the chemorepellent force takes place with an elongated shape due to low/high cell density extrema. Actually, in the same way as previously explained, cells move faster when they encounter low density

either of fibres or of cells. Then a non-symmetric high density corolla surrounding the hole appears. In a second step, again the diffusive mechanisms homogenize the corolla to finish at the axi-symmetric stationary state.



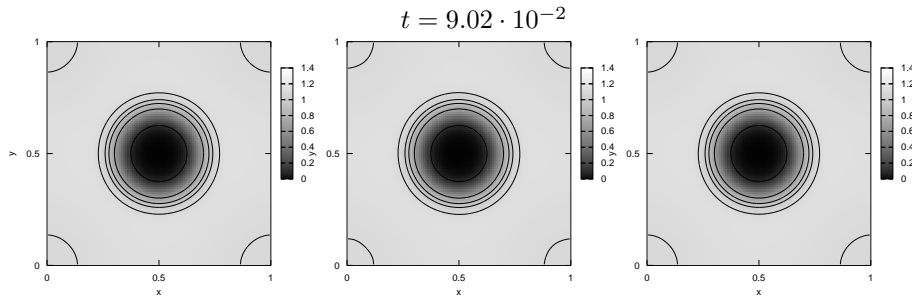


FIGURE 3. Evolution of the cell density contours for the three cases detailed in the text: totally homogeneous case (left column), inhomogeneity of the ECM (central column), inhomogeneous initial cell density in a homogeneous ECM (right column).

To close this first numerical study, Figure 4 shows the stationary solution that is the same in the three studied cases and is always obtained for large times.

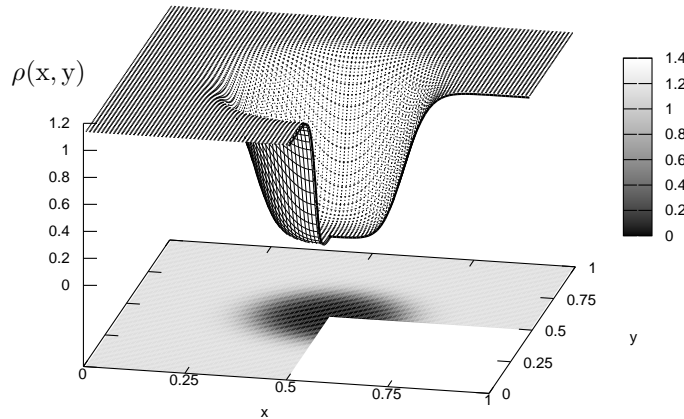


FIGURE 4. Comparison between the two-dimensional stationary solutions obtained numerically in the three cases of Fig.3, and the radially symmetric analytical solution plotted in bold.

With regard to the second set of simulations, we consider the motion induced by a constant chemotactic force $\mathbf{f} = \mathbf{e}_x$ and it will be shown how either inhomogeneity or anisotropy of the ECM influences the motion. The two first examples focus on the inhomogeneity of the ECM, treated here as an obstacle modeled by a local increase of the fibre density shown in Figure 5. The situation is studied in the isotropic configuration ($\mathbb{D} = \mathbb{I}$) for small and high Peclet numbers, and for the value $\alpha = 1$. Specificities of the motion are presented in both cases.

The behavior of the cell density differs in the two simulations. First of all, considering the high Peclet number case presented in Figure 6, one can observe that the motion toward the right of the domain is very fast, due to the importance of the taxis compared to the random-walk motion: diffusion-like motion is present but not important.

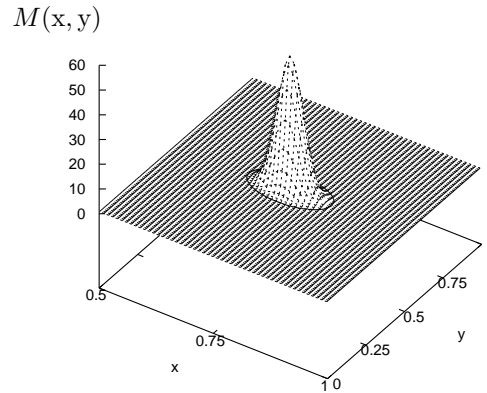


FIGURE 5. Gaussian distribution of the fibre density corresponding to the simulations shown in Figs.6 and 7. The bold contour curve corresponds to the value 1 and is also plotted as a reference in the following evolution graphs.

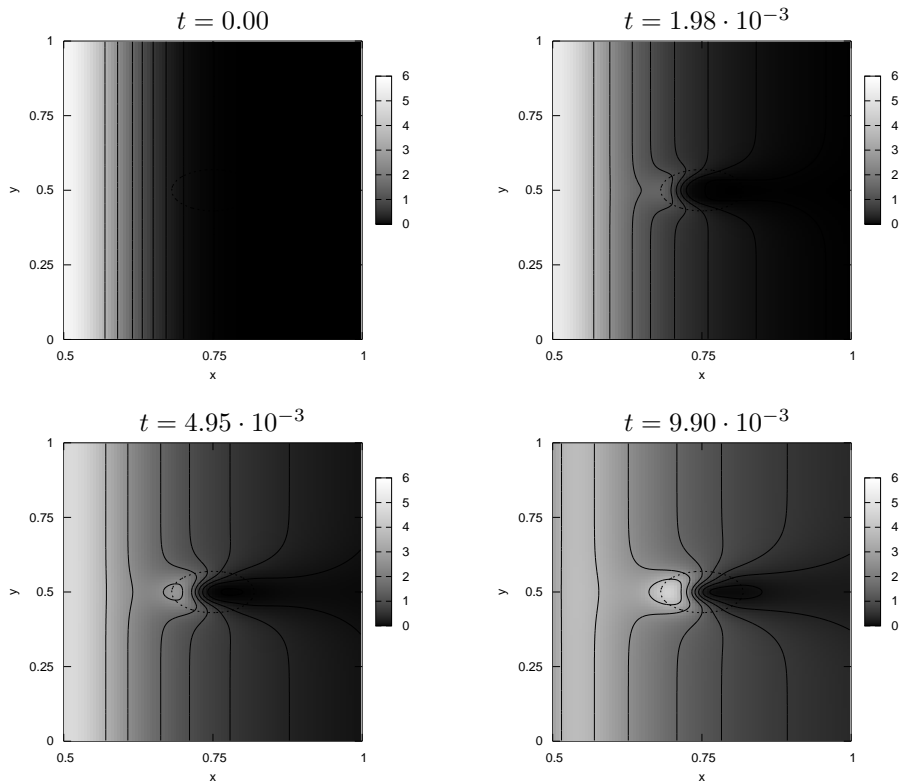


FIGURE 6. Cell density evolution in an inhomogeneous ECM at high Peclet number ($\mathcal{P}_e = 50$). The dot-plotted curve corresponds to the value $M(x, y) = 1$.

When arriving at the locally high density of fibres, cells begin to strongly accumulate just in front of the obstacle while they continue their own motion normally

if far enough from this obstacle, i.e. at the top and the bottom of the domain: the chemotactic force is strong enough to avoid the random-walk effect in motion, that could be a way to circumvent the obstacle. The deformation of the level contours (originally straight) close to the high fibre density also shows that cells just upon or under the obstacle succeed in passing easier. In the second half part of the ellipsoid shown on each graph - which indicates the location of the increased fibre density - a dim area remains and shows that cells cannot pass through the obstacle. While cells continue to move toward the right, at the bottom and the top of the domain, a dimmer elongated area can be observed behind the ellipsoid, showing that the chemotactic force is strong enough to attract the cells to the right, without letting them the time to random-walk and close the hole in the cell density created behind the obstacle.

When looking at the small Peclet number simulation shown in Figure 7, the behavior is quite different.

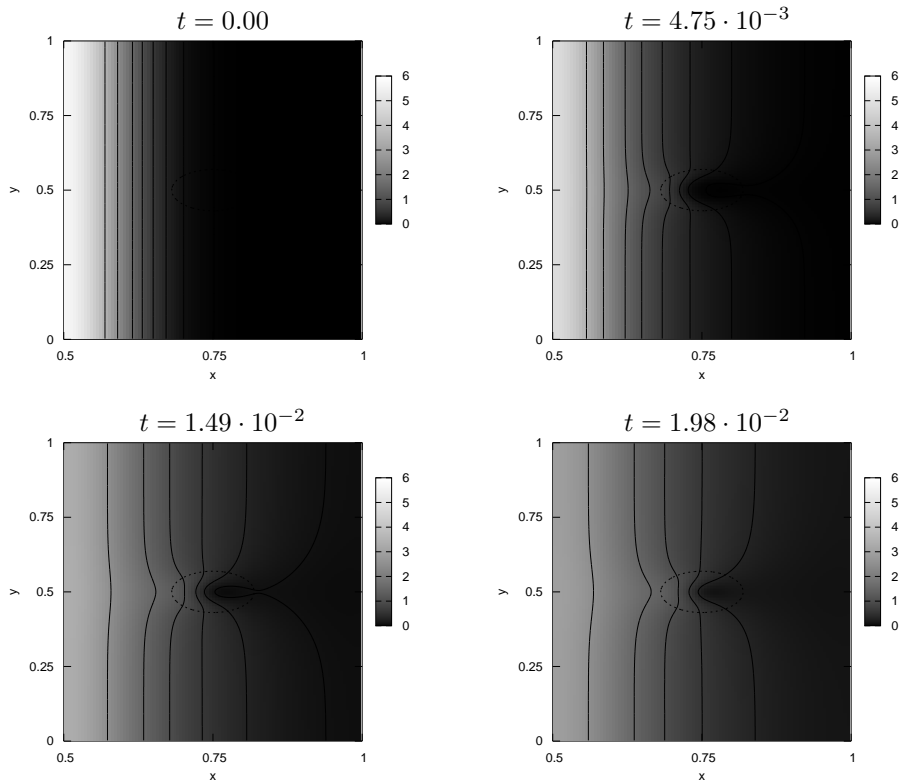


FIGURE 7. Cell density evolution in an inhomogeneous ECM at low Peclet number ($\mathcal{P}_e = 0.02$). The dot-plotted curve corresponds to the value $M(x, y) = 1$.

Actually, the motion is less fast toward the right of the domain, due to the importance of the random-walk motion compared to the taxis. The accumulation in front of the obstacle is weak, because cells have time to circumvent the obstacle and continue their motion afterwards. Note that in the second half part of the ellipsoid again a dim area remains. However this hole in the cell density is quite

small and tends to be filled up by cells random-walking when the chemotactic force is not so strong.

So by these two cases, we show that the influence of inhomogeneities of the ECM is not only to slow down the motion, but also to modify its direction. According to the value of the Peclet number, we exhibited two clear behaviors in the cell motion: Accumulating or circumventing.

After having presented motions diversely affected by the inhomogeneities of the ECM, we want to focus on a specific anisotropic case. We conserve the configuration used in the last two simulations considering a constant chemoattractive force toward the right of the domain. However we deal now with an homogenous distribution of the fibres, while their orientation may depend on the location in the domain. More precisely, fibres are orientation-distributed in a way such that the orientation tensor \mathbb{D} is diagonal and written as

$$\mathbb{D}(\mathbf{x}) = \begin{pmatrix} D(x,y) & 0 \\ 0 & 2 - D(x,y) \end{pmatrix}. \quad (89)$$

We present in Fig.8 the evolution in space of the coefficient D .

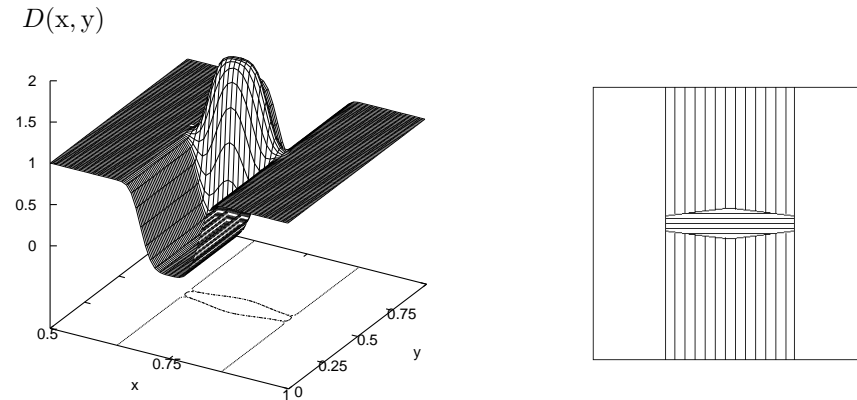


FIGURE 8. Evolution in space of the anisotropy coefficient D - contours plotted at the bottom show the different areas of anisotropy in the physical domain - (left) and corresponding schematic representation of the fibres orientation in the anisotropic areas (right).

When D is equal to one, the distribution of the ECM fibres is locally isotropic. On the contrary, if the value of D is close to zero in one point, then the ECM is locally anisotropic and the main orientation of the network in this point is the y -direction. Respectively, if the value of D is close to two in one point, then the ECM is also locally anisotropic but the main orientation of the network is then the x -direction. So we propose the following anisotropic configuration: the domain is generally isotropic, but contains an area in the y -direction (see Fig.8) in which the isotropy is lost. At the top and the bottom of this area, the fibres are mainly oriented along y (perpendicularly to the chemoattractive force) while in the central zone the orientation is mainly along x , in the direction of the chemoattractive force.

Two phenomena can be observed in Figure 9 depending on where cells join the vertical anisotropic area. In the central part, cells accelerate toward the right because x -motion is easier along the x -oriented fibres. On the contrary, near the

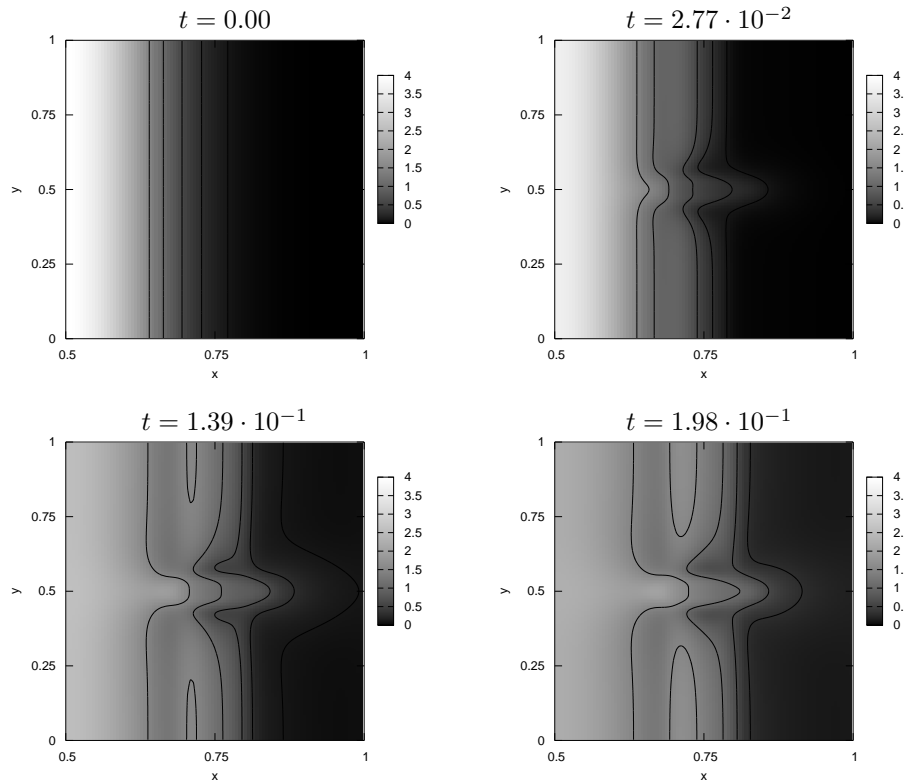


FIGURE 9. Cell density evolution in a homogeneous and anisotropic ECM. Parameters are $\mathcal{P}_e = 1$ and $\alpha = 0.5$.

bottom and the top of the domain, cells slow down in their x-motion because they encounter fibres perpendicular to their motion. So a central finger-like shape appears as a deformation of the level curves, which shows an easier and faster motion toward the right of the domain. On the contrary, two symmetric accumulation areas appear where fibres begin to align in y.

8. Conclusion. In order to describe cell motion in extracellular matrix taking into account of cell-cell and cell-matrix interactions, and degradation of the ECM fibres in addition to chemotaxis and haptotaxis, we proposed a kinetic and a diffusion model, studying the relation between the mesoscopic and the macroscopic configuration.

In a first step, only the macroscopic model is studied numerically. It is shown how the solution tends toward the analytical stationary configuration and how it behaves in an anisotropic or heterogeneous ECM distribution. For instance, we exhibited that, according to the respective influence of the chemotaxis and of the random motion, cells tend either to circumvent (if possible) high fibre density regions or accumulate in these regions. It is also shown how a local anisotropy of the ECM changes the cell motion according to the main direction of the fibres. In a future work, we will compare simulations of the mesoscopic model with simulations of the macroscopic one.

The modeling approach is a first step toward the modeling of cell motion in a fibrous structure. The validity of the model is now evaluated with some in vitro experiments in a two-dimensional setup, so that the encounter rates and the transition probabilities can be evaluated. From the modeling point of view it would be very interesting to include a possible dependence on the density or on the velocity of the cells and to obtain volume filling or quorum sensing models [24].

To conclude, the present models include a possible remodeling of the surrounding network tissue by adding fibre degradation to the cell motion equation. It is worth mentioning that remodeling should also include the generation of new fibres in the main direction of cell motion.

REFERENCES

- [1] W. Alt, *Singular perturbation of differential integral equations describing biased random walks*, J. reine angew. Math., **322** (1981), 15–41.
- [2] D. Ambrosi, *Cellular traction as an inverse problem*, SIAM J. Appl. Math, **66** (2006), 2049–2060.
- [3] D. Ambrosi, F. Bussolino and L. Preziosi, *A review of vasculogenesis models*, J. Theor. Med., **6** (2005), 1–19.
- [4] L. Arlotti, N. Bellomo, E. De Angelis and M. Lachowicz, “Generalized Kinetic Models in Applied Sciences,” World Scientific, Singapore, 2003.
- [5] A. Bellouquid and M. Delitala, “Mathematical Modeling of Complex Biological Systems: A Kinetic Theory Approach,” Birkhauser, 2006.
- [6] C. Cercignani, R. Illner and M. Pulvirenti, “The Mathematical Theory of Dilute Gases,” Springer, New York, 1994.
- [7] F. A. C. C. Chalub, P. A. Markowich, B. Perthame and C. Schmeiser, *Kinetics models for chemotaxis and their drift-diffusion limits*, Monatsh. Math., **142** (2004), 123–141.
- [8] A. Chauviere, T. Hillen and L. Preziosi, *Modeling the motion of a cell population in the extracellular matrix*, to appear in Discr. Cont. Dyn. Syst. (2007).
- [9] M. Dembo and Y. L. Wang, *Stresses at the cell-to-substrate interface during locomotion of fibroblasts*, Biophysical J., **76** (1999), 2307–2316.
- [10] R. B. Dickinson, *A model for cell migration by contact guidance*, in W. Alt, A. Deutsch and G. Dunn editors, “Dynamics of Cell and Tissue Motion,” Basel, Birkhauser, (1997), 149–158.
- [11] R. B. Dickinson, *A generalized transport model for biased cell migration in an anisotropic environment*, J. Math. Biol., **40** (2000), 97–135.
- [12] R. B. Dickinson, S. Guido and R. T. Tranquillo, *Biased cell migration of fibroblasts exhibiting contact guidance in oriented collagen gels*, Biomedical and Life Sciences, **22** (1994), 342–356.
- [13] R. B. Dickinson and R. T. Tranquillo, *A stochastic model for cell random motility and haptotaxis based on adhesion receptor fluctuations*, J. Math. Biol., **31** (1993), 563–600.
- [14] R. B. Dickinson and R. T. Tranquillo, *Transport equations and cell movement indices based on single cell properties*, SIAM J. Appl. Math., **55** (1995), 1419–1454.
- [15] F. Filbet, P. Laurençot and B. Perthame, *Derivation of hyperbolic models for chemosensitive movement*, J. Math. Biol., **50** (2005), 189–207.
- [16] P. Friedl, *Prespecification and plasticity: shifting mechanisms of cell migration*, Curr. Opin. Cell. Biol., **16** (2004), 14–23.
- [17] P. Friedl and E. B. Bröcker, *The biology of cell locomotion within three dimensional extracellular matrix*, Cell Motility Life Sci., **57** (2000), 41–64.
- [18] P. Friedl and K. Wolf, *Tumour-cell invasion and migration: diversity and escape mechanisms*, Nature Rev., **3** (2003), 362–374.
- [19] A. Gamba, D. Ambrosi, A. Coniglio, A. de Candia, S. Di Talia, E. Giraud, G. Serini, L. Preziosi and F. Bussolino, *Percolation, morphogenesis and Burgers dynamics in blood vessels formation*, Phys. Rev. Lett., **90** (2003), 118101/1–4.
- [20] E. Geigant, *On peak and periodic solutions of an integro-differential equation on S^1* , in “Geometric Analysis and Nonlinear Partial Differential Equations,” Springer Berlin, (2003), 463–474.
- [21] T. Hillen, *(M5) Mesoscopic and macroscopic models for mesenchymal motion*, J. Math. Biol., **53** (2006), 585–616.

- [22] T. Hillen and H. G. Othmer, *The diffusion limit of transport equations derived from velocity jump processes*, SIAM J. Appl. Math., **61** (2000), 751–775.
- [23] V. Lanza, D. Ambrosi and L. Preziosi, *Exogenous control of vascular network formation in vitro: A mathematical model*, Networks and Heterogeneous Media, **1** (2006).
- [24] K. Painter and T. Hillen, *Volume-filling and quorum sensing in models for chemosensitive movement*, Canadian Applied Mathematics Quarterly, **10** (2002), 501–543.
- [25] K. Painter, *Mathematical modelling of individual cell migration strategies in the extracellular matrix*, submitted in J. Math. Biol., (2007).
- [26] G. Serini, D. Ambrosi, E. Giraudo, A. Gamba, L. Preziosi and F. Bussolino, *Modeling the early stages of vascular network assembly*, EMBO J., **22** (2003), 1771–1779.
- [27] A. Tosin, D. Ambrosi and L. Preziosi, *Mechanics and chemotaxis in the morphogenesis of vascular networks*, Bull. Math. Biol., **68** (2006), 1819–1836.
- [28] R. T. Tranquillo and V. H. Barocas, *A continuum model for the role of fibroblast contact guidance in wound contraction*, in “Dynamics of Cell and Tissue Motion” (eds: W. Alt, A. Deutsch and G. Dunn), Basel, Birkhauser, (1997), 159–164.
- [29] K. Wolf, I. Mazo, H. Leung, K. Engelke, U. H. von Andrian, E. I. Deryugina, A. Y. Strongin, E. B. Bröcker and P. Friedl, *Compensation mechanism in tumor cell migration: mesenchymal–ameboid transition after blocking of pericellular proteolysis*, J. Cell. Biol., **160** (2003), 267–277.

Received December 2006; revised March 2007.

E-mail address: `chauviere@calvino.polito.it`

E-mail address: `thillen@ualberta.ca`

E-mail address: `luigi.preziosi@polito.it`